

Adiabatic approximation in the ultrastrong-coupling regime of a system consisting of an oscillator and two qubits

Ping Yang, Zhi-Ming Zhang*

*Laboratory of Nanophotonic Functional Materials and Devices,
SIPSE and LQIT, South China Normal University, Guangzhou 510006, China*

(Dated: August 8, 2018)

Abstract

We present a system composed of two flux qubits and a transmission-line resonator. Instead of using the rotating wave approximation (RWA), we analyse the system by the adiabatical approximation methods under two opposite extreme conditions. Basic properties of the system are calculated and compared under these two different conditions. Energy-level spectrum of the system in the adiabatical displaced oscillator basis is shown, and the theoretical result is compared with the numerical solution.

PACS numbers: 42.50.-p, 42.50.Dv, 85.25.Cp

* Corresponding author's email address: zmzhang@scnu.edu.cn

I. INTRODUCTION

Recently, more and more attention has been paid to superconducting devices [1–6] to build quantum systems, as the tunability of system parameters, which is one of the most exciting advantages of superconducting circuit QED over natural-particle-based cavity QED, makes such devices more likely to be successful in quantum information processing [7–9]. In fact, some remarkable progresses have been made in recent years, such as Fock states preparation in superconducting devices [10], single-photon router in the microwave regime [11], and high-fidelity readout in circuit QED [12]. Superconducting flux qubit that consists of superconducting loops and Josephson junctions can be viewed as a two-level system when the parameters satisfy the condition called degeneracy point [13].

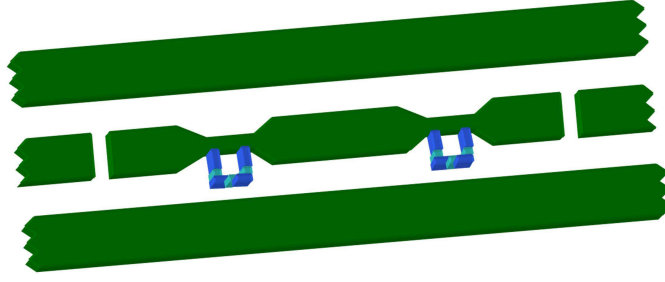
The paper is organized as follows: In Sec. II we introduce the system and the Hamiltonian. In Sec. III we discuss the properties of the system by adiabatic approximation under two opposite extreme conditions. Energy-level spectrum of the system in the adiabatical displaced oscillator basis is shown, and the theoretical result is compared with the numerical solution. Sec. IV is the conclusion.

II. SYSTEM AND HAMILTONIAN

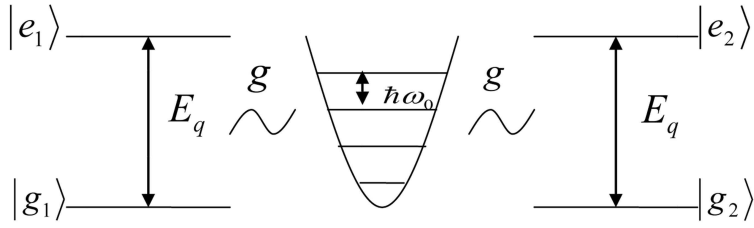
The system that we consider consists of a harmonic oscillator and two three-Josephson-junction qubits (The smallest junction has been replaced by an additional loop [14]) which are coupled to the oscillator. Hamiltonian of such qubit is given by \hat{H}_{q_i} in Eq. (2).

The oscillator here is a microwave transmission-line resonator, and the qubits which are superconducting flux qubits are fabricated so that the loops are closed by the center conductor [15]. The schematic diagram of the structure is shown in Fig. 1(a), and it is worth noting that the distance between the two qubits is sufficient large such that the interaction between them can be ignored. The schematic graph of our system is illustrated in Fig. 1(b), in which two qubits are coupled to a harmonic oscillator. It is worth noting that the qubits are considered to be identical, which means that the parameters Δ , ϵ , E_q , and the coupling strength g for both of the qubits are of the same value.

The Hamiltonian corresponding to our system is



(a)



(b)

FIG. 1. (Color online) (a) Schematic diagram of the structure. The two light blue squares are improved three-junction flux qubits fabricated to the center conductor. (b) Schematic graph of the system. Two identical qubits (i.e. parameters Δ , ϵ , energy-level splitting E_q and coupling strength g for both qubits are of the same value) viewed as two-level system with ground state $|g\rangle$ and excited state $|e\rangle$, are coupled to a harmonic oscillator whose characteristic frequency is ω_0 .

$$\hat{H} = \sum_{i=1,2} \hat{H}_{q_i} + \hat{H}_{os} + \hat{H}_{int}, \quad (1)$$

where

$$\begin{aligned} \hat{H}_{q_i} &= -\frac{\Delta}{2} \hat{\sigma}_{x_i} - \frac{\epsilon}{2} \hat{\sigma}_{z_i}, \\ \hat{H}_{os} &= \frac{\hat{p}^2}{2m} + \frac{1}{2} m \omega_0^2 \hat{x}^2, \\ \hat{H}_{int} &= g \hat{x} (\hat{\sigma}_{z_1} + \hat{\sigma}_{z_2}), \end{aligned} \quad (2)$$

where Δ is the energy gap tuned by the flux in the additional loop, and ϵ is the bias tuned by magnetic flux in the main loop. Energy-level splitting $E_q = \sqrt{\Delta^2 + \epsilon^2}$, and it will be useful for the following analysis to define an angle θ by $\tan \theta = \epsilon/\Delta$. \hat{p} and \hat{x} are the

momentum operator and position operator of the harmonic oscillator. $\hat{\sigma}_{x_i}$ and $\hat{\sigma}_{z_i}$ are the Pauli operators of the i th qubit.

We express the Hamiltonian of the oscillator and interaction using \hat{a}^\dagger and \hat{a} (creation and annihilation operator of the oscillator), so \hat{H}_{os} and \hat{H}_{int} are rewritten as

$$\begin{aligned}\hat{H}_{os} &= \hbar\omega_0\hat{a}^\dagger\hat{a} + \frac{1}{2}\hbar\omega_0, \\ \hat{H}_{int} &= \lambda(\hat{a}^\dagger + \hat{a})(\hat{\sigma}_{z_1} + \hat{\sigma}_{z_2}), \\ \lambda &= \sqrt{\frac{\hbar}{2m\omega_0}}g.\end{aligned}\tag{3}$$

There is no analytic solution to Eq. (1) so far, but some approximation methods have been discussed for one-qubit case without RWA (such as [16], [17]). In the next section, we present two adiabatic approximations that can be used to describe our system under different regimes of parameters.

III. ADIABATIC APPROXIMATIONS UNDER TWO OPPOSITE EXTREME CONDITIONS

A. Adiabatic approximation in the displaced oscillator basis

In this section we consider the case in which $\hbar\omega_0$ is far greater than E_q . In this case, using adiabatic approximation, one can consider that each of the qubits has a well-defined value of σ_z , i.e., $\sigma_{z_1} = \pm 1$, and $\sigma_{z_2} = \pm 1$ [18]. When $\sigma_{z_1} = \sigma_{z_2} = \pm 1$, eigenstates of the system can be written as $|\psi_\pm, \pm\rangle = |\psi_\pm\rangle \otimes |\pm\rangle$, where $|\psi_\pm\rangle$ stand for eigenstates of the oscillator, $|+\rangle$ and $|-\rangle$ stand for the qubits' eigenstates $|e_1, e_2\rangle$ and $|g_1, g_2\rangle$, respectively. When $\sigma_{z_1} = -\sigma_{z_2} = \pm 1$, eigenstates of the system can be written as $|\psi_0, 0\rangle = |\psi_0\rangle \otimes |0\rangle$, where $|0\rangle$ stands for $|e_1, g_2\rangle$ and $|g_1, e_2\rangle$.

In the case $\sigma_{z_1} = \sigma_{z_2} = \pm 1$ which means the states of qubits are $|e_1, e_2\rangle$ or $|g_1, g_2\rangle$, the effective Hamiltonian of the oscillator [19]

$$\hat{H}_{os,eff}|_{\sigma_{z_1}=\sigma_{z_2}=\pm 1} = \hbar\omega_0\hat{a}^\dagger\hat{a} \pm 2\lambda(\hat{a} + \hat{a}^\dagger).\tag{4}$$

Assuming λ and ω_0 are all real, eigenstates of this Hamiltonian are as follows which can be viewed as displaced Fock states:

$$|\psi_\pm\rangle = e^{\mp(2\lambda/\hbar\omega_0)(\hat{a}^\dagger - \hat{a})}|n\rangle = |n_\pm\rangle, \quad n = 0, 1, 2, \dots,\tag{5}$$

The eigenenergies are given by

$$E'_{n_{\pm}} = n\hbar\omega_0 - 4\lambda^2/\hbar\omega_0, \quad n = 0, 1, 2, \dots \quad (6)$$

In the case $\sigma_{z_1} = -\sigma_{z_2} = \pm 1$ which means states of qubits are $|e_1, g_2\rangle$ or $|g_1, e_2\rangle$, the effective Hamiltonian of the oscillator is the same as the usual harmonic oscillator

$$\hat{H}_{os,eff}|_{\sigma_{z_1}=-\sigma_{z_2}=\pm 1} = \hbar\omega_0(\hat{a}^\dagger\hat{a} + 1/2). \quad (7)$$

So the eigenstates are given by Fock states

$$|\psi_0\rangle = |n\rangle = |n_0\rangle, \quad n = 0, 1, 2, \dots, \quad (8)$$

and eigenenergies are given by

$$E'_{n_0} = \hbar\omega_0(n + 1/2) \quad n = 0, 1, 2, \dots \quad (9)$$

The eigenstates and eigenenergies obtained by Eqs. (5), (6), (8), and (9) build the main results of displaced oscillator basis, which will be used throughout the following analysis. The potentials corresponding to above results are harmonic oscillator potentials which are illustrated by Fig. 2.

Because the eigenstates of the oscillator depend on the states of qubits now, there will be some new properties of the oscillator's states. States of the same potential well (presented in Fig. 2) still maintain the usual orthonormality, that is $\langle m_+|n_+\rangle = \delta_{mn}$, $\langle m_0|n_0\rangle = \delta_{mn}$, $\langle m_-|n_-\rangle = \delta_{mn}$, while states of different potential wells do not, the displacement operator cause a displacement in x , so they are no longer orthogonal to each other. The overlaps between displaced oscillator basis of different wells are given by

$$\langle m_-|n_0\rangle = \begin{cases} e^{-2\lambda^2/\hbar^2\omega_0^2} (-2\lambda/\hbar\omega_0)^{m-n} \sqrt{n!/m!} L_n^{m-n} [(2\lambda/\hbar\omega_0)^2], & m \geq n, \\ e^{-2\lambda^2/\hbar^2\omega_0^2} (2\lambda/\hbar\omega_0)^{n-m} \sqrt{m!/n!} L_m^{n-m} [(2\lambda/\hbar\omega_0)^2], & m < n, \end{cases} \quad (10)$$

$$\langle m_0|n_+\rangle = \begin{cases} e^{-2\lambda^2/\hbar^2\omega_0^2} (-2\lambda/\hbar\omega_0)^{m-n} \sqrt{n!/m!} L_n^{m-n} [(2\lambda/\hbar\omega_0)^2], & m \geq n, \\ e^{-2\lambda^2/\hbar^2\omega_0^2} (2\lambda/\hbar\omega_0)^{n-m} \sqrt{m!/n!} L_m^{n-m} [(2\lambda/\hbar\omega_0)^2], & m < n, \end{cases} \quad (11)$$

and

$$\langle m_-|n_+\rangle = \begin{cases} e^{-4\lambda^2/\hbar^2\omega_0^2} (-4\lambda/\hbar\omega_0)^{m-n} \sqrt{n!/m!} L_n^{m-n} [(4\lambda/\hbar\omega_0)^2], & m \geq n, \\ e^{-4\lambda^2/\hbar^2\omega_0^2} (4\lambda/\hbar\omega_0)^{n-m} \sqrt{m!/n!} L_m^{n-m} [(4\lambda/\hbar\omega_0)^2], & m < n, \end{cases} \quad (12)$$

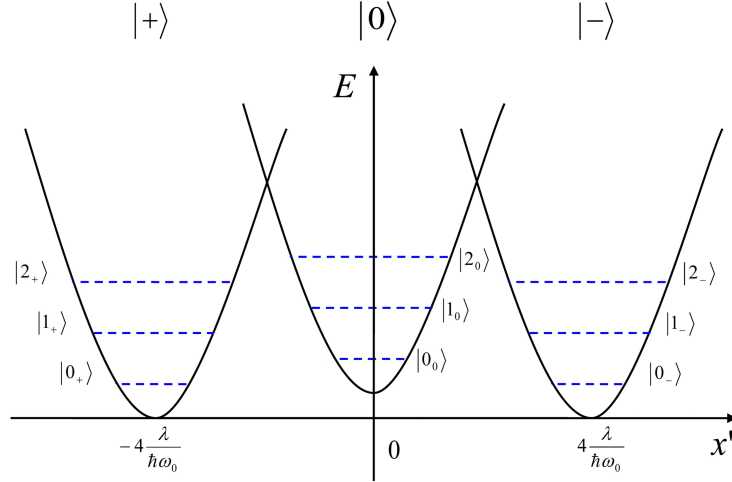


FIG. 2. (Color online) Schematic diagram of the displaced oscillator basis. The horizontal axis $x' = x\sqrt{\frac{2m\omega_0}{\hbar}}$. All three wells maintain the same harmonic character, and usual eigenstates as well. The equilibrium position of the left (or the right) well is shifted by a specific constant. The shift direction is to the left (or right) when the qubits are in $|+\rangle = |e_1, e_2\rangle$ (or $|-\rangle = |g_1, g_2\rangle$). The middle potential well which is double degenerate corresponds to non-displaced case in which the states of the two qubits are opposite, i.e., $|0\rangle$, and the equilibrium position is higher than the others. Eigenstates which have the same value of n in the left are degenerate with the right well in energy.

where L_m^n are the associated Laguerre polynomials. It is worth noting that $\langle m_0|n_-\rangle = (-1)^{m-n}\langle m_-|n_0\rangle$, and $\langle m_+|n_0\rangle = (-1)^{m-n}\langle m_0|n_+\rangle$, which are useful identities in the later calculation.

Having obtained the eigenstates of the displaced oscillator together with their properties, we now focus on the qubits. Taking any specific value of n , one can build an effective Hamiltonian of the qubits for that value of n . Due to the fact that for each value of n there are four qubits' states, namely $|e_1, e_2\rangle$, $|e_1, g_2\rangle$, $|g_1, e_2\rangle$, and $|g_1, g_2\rangle$, the matrix of the effective Hamiltonian of qubits is a 4×4 matrix in the space defined by $|n_+, e_1, e_2\rangle$, $|n_0, e_1, g_2\rangle$, $|n_0, g_1, e_2\rangle$, and $|n_-, g_1, g_2\rangle$. Based on the overlaps between displaced oscillator basis obtained previously, we can calculate the elements of this matrix immediately, and the

matrix is given by

$$\hat{\mathbf{H}}_{\mathbf{q},\text{eff}} = \begin{pmatrix} -\epsilon & -\frac{\Delta}{2}\langle n_+|n_0\rangle & -\frac{\Delta}{2}\langle n_+|n_0\rangle & 0 \\ -\frac{\Delta}{2}\langle n_0|n_+\rangle & 0 & 0 & -\frac{\Delta}{2}\langle n_0|n_-\rangle \\ -\frac{\Delta}{2}\langle n_0|n_+\rangle & 0 & 0 & -\frac{\Delta}{2}\langle n_0|n_-\rangle \\ 0 & -\frac{\Delta}{2}\langle n_-|n_0\rangle & -\frac{\Delta}{2}\langle n_-|n_0\rangle & \epsilon \end{pmatrix}, \quad (13)$$

where $\langle n_+|n_0\rangle$, $\langle n_0|n_+\rangle$, $\langle n_-|n_0\rangle$ and $\langle n_0|n_-\rangle$ are calculated to be of the same value as $e^{-2(\lambda/\hbar\omega_0)^2} L_n(4\lambda^2/\hbar\omega_0^2)$.

Eigenenergies of this effective Hamiltonian are given by

$$\begin{aligned} E''_{n_{\pm}} &= \pm \sqrt{\epsilon^2 + \Delta^2 [e^{-2(\lambda/\hbar\omega_0)^2} L_n(4\lambda^2/\hbar\omega_0^2)]^2}, \\ E''_{n_0} &= 0, \\ n &= 0, 1, 2, \dots \end{aligned} \quad (14)$$

and eigenstates are given by

$$\begin{aligned} |\psi_{n-}\rangle &= \left(1 + 2\Theta_n^2 + 2\Theta_n\sqrt{1 + \Theta_n^2}\right) |n_+, e_1, e_2\rangle + |n_-, g_1, g_2\rangle \\ &\quad + \left(\Theta_n + \sqrt{1 + \Theta_n^2}\right) |n_0, e_1, g_2\rangle + \left(\Theta_n + \sqrt{1 + \Theta_n^2}\right) |n_0, g_1, e_2\rangle, \\ |\psi_{n_0_1}\rangle &= -|n_+, e_1, e_2\rangle + |n_-, g_1, g_2\rangle + 2\Theta_n |n_0, e_1, g_2\rangle, \\ |\psi_{n_0_2}\rangle &= -|n_0, e_1, g_2\rangle + |n_0, g_1, e_2\rangle, \\ |\psi_{n+}\rangle &= \left(1 + 2\Theta_n^2 - 2\Theta_n\sqrt{1 + \Theta_n^2}\right) |n_+, e_1, e_2\rangle + |n_-, g_1, g_2\rangle \\ &\quad + \left(\Theta_n - \sqrt{1 + \Theta_n^2}\right) |n_0, e_1, g_2\rangle + \left(\Theta_n - \sqrt{1 + \Theta_n^2}\right) |n_0, g_1, e_2\rangle, \end{aligned} \quad (15)$$

where $\Theta_n = \frac{\tan \theta}{e^{-2(\lambda/\hbar\omega_0)^2} L_n(4\lambda^2/\hbar\omega_0^2)}$.

The energies of the system are drawn as $E_{n_{\pm}} = E'_{n_{\pm}} + E''_{n_{\pm}}$ and $E_{n_0} = E'_{n_0} + E''_{n_0}$. We present the energy-level spectrum as a function of $\lambda/\hbar\omega_0$ in Fig. 3, and these four pictures are different in θ . It is obvious that no matter how we set the regime of the parameters, E_{n_0} remain constant for any specific value of n , so we do not present these horizontal lines in the figures. All of the four diagrams are under the condition that $\hbar\omega_0/E_q = 4$ to ensure the adiabatical approximation. When $\lambda = 0$, energy levels of the system are simplified to $n\hbar\omega + E_q$ which are different from the energy-levels of the usual harmonic oscillator by a constant, so they are equally spaced. As λ increases, behaviors are evidently different for different value of θ . In the case $\theta = 0$ (i.e. qubits are in the degenerate point), when λ increases, some slight avoided crossing emerges, and in the limit of large λ the levels which

have the same value of n form pairs. In the case $\theta = \pi/6$, avoided crossing vanishes and splitting of energy-level pairs with the same value of n turns up in the large λ limit. The splitting of energy pairs enhances when $\theta = \pi/4$. In the case $\theta = \pi/3$, there is no obvious energy pairs any more, and space between each energy levels maintain the same in the duration of increasing λ .

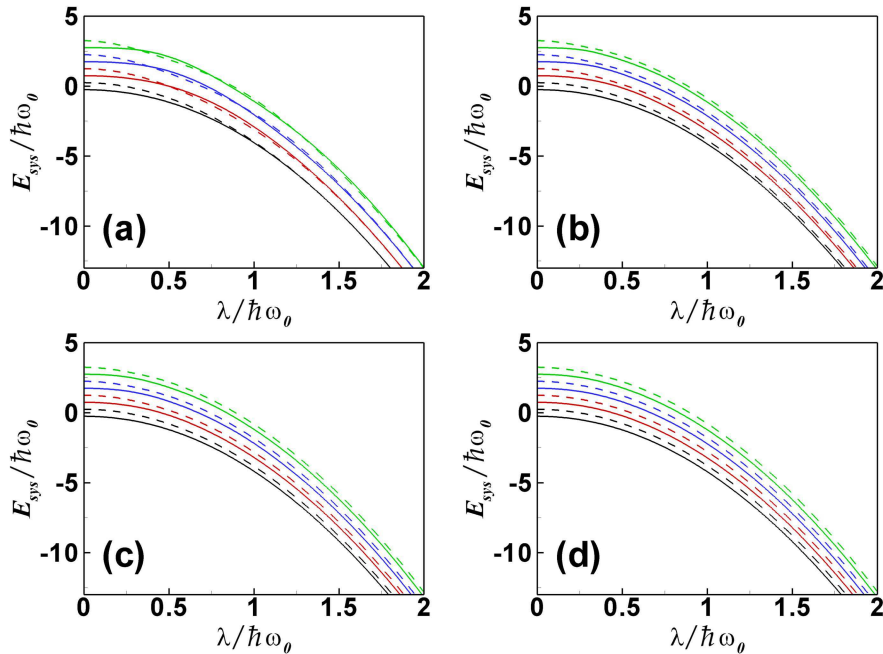


FIG. 3. (Color online) The energy-level spectrum diagram of several lower levels as a function of $(\lambda/\hbar\omega_0)$. $\hbar\omega_0/E_q = 4$. The different color denotes different states of the oscillator (black for $n = 0$, red for $n = 1$, blue for $n = 2$, and green for $n = 3$). The solid lines stand for qubits in state $|g_1, g_2\rangle$, and the dashed lines stand for $|e_1, e_2\rangle$. (a) $\theta = 0$, in the limit of large λ the levels which have the same value of n form pairs. (b) $\theta = \pi/6$, avoided crossing vanishes and splitting of energy-level pairs with the same value of n turns up in the large λ limit. (c) $\theta = \pi/4$, splitting of energy pairs enhances. (d) $\theta = \pi/3$, there is no obvious energy pairs any more, and space between each energy levels maintains the same in the duration of increasing λ .

We show the comparison between the displaced oscillator adiabatical approximation method which is given by Eq. (14) and the numerical solution for several lower levels in Fig. 4. They fit well in almost all regime of λ .

When the qubits are in the degeneracy point, i.e., $\epsilon = 0$, the states of the system corresponding to the energies E_{n-} , E_{n_0} (double degenerate) and E_{n+} are superposition states of

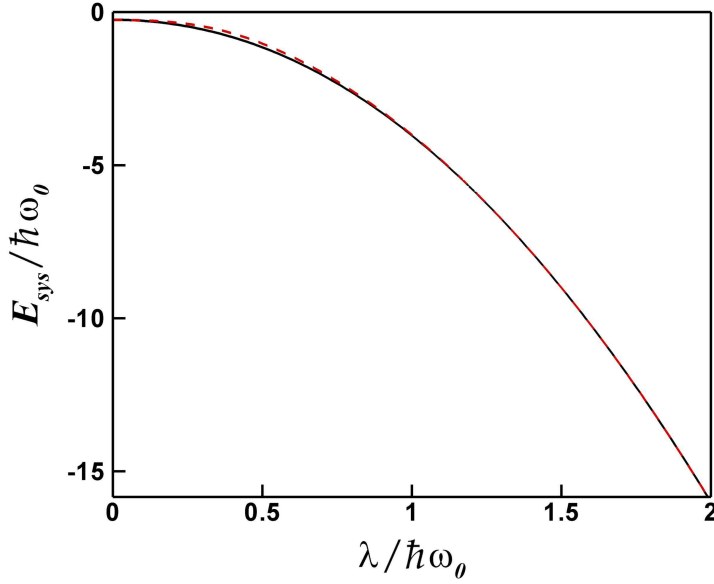


FIG. 4. (Color online) The comparison between the displaced oscillator adiabatic approximation and the numerical solution for the lowest energy level. They fit well in almost all regime of λ .

the displaced basis, which are given by

$$\begin{aligned}
 |\psi_{n_-}\rangle &= 1/4|n_+, e_1, e_2\rangle + 1/4|n_0, e_1, g_2\rangle + 1/4|n_0, g_1, e_2\rangle + 1/4|n_-, g_1, g_2\rangle, \\
 |\psi_{n_{01}}\rangle &= -1/\sqrt{2}|n_+, e_1, e_2\rangle + 1/\sqrt{2}|n_-, g_1, g_2\rangle, \\
 |\psi_{n_{02}}\rangle &= -1/\sqrt{2}|n_0, e_1, g_2\rangle + 1/\sqrt{2}|n_0, g_1, e_2\rangle, \\
 |\psi_{n_+}\rangle &= 1/4|n_+, e_1, e_2\rangle - 1/4|n_0, e_1, g_2\rangle - 1/4|n_0, g_1, e_2\rangle + 1/4|n_-, g_1, g_2\rangle.
 \end{aligned} \tag{16}$$

It is interesting that no matter how we set the regime of the parameters, $|\psi_{n_{02}}\rangle$ always has the form mentioned in Eqs. (15)-(16). It can be rewritten as $|\psi_{n_{02}}\rangle = 1/\sqrt{2}(-|e_1, g_2\rangle + |g_1, e_2\rangle) \otimes |n_0\rangle$, which means that oscillator is decoupled to the states of the qubits. So the two-qubit maximally entangled states can be obtained by detecting the state of the oscillator.

B. Adiabatic approximation for the case of high-frequency qubits

In this section we consider the case that E_q is far larger than $\hbar\omega_0$. In this case, similar to what we have discussed above, using adiabatic approximation one can consider that the oscillator has a well-defined value of x [18]. Thus the effective Hamiltonian of the qubits is

[19]

$$\hat{H}_{q,eff}|x\rangle = -\frac{\Delta}{2}(\hat{\sigma}_{x_1} + \hat{\sigma}_{x_2}) - \frac{\epsilon}{2}(\hat{\sigma}_{z_1} + \hat{\sigma}_{z_2}) + gx(\hat{\sigma}_{z_1} + \hat{\sigma}_{z_2}). \quad (17)$$

The eigenenergies of Eq. (17) are given by

$$\begin{aligned} E_{q\pm} &= \pm\sqrt{\Delta^2 + (2gx - \epsilon)^2}, \\ E_{q_0} &= 0, \quad (\text{double degenerate}) \end{aligned} \quad (18)$$

Unlike above results that energies of high-frequency oscillator are independent of the qubits' states, the energies of high-frequency qubits now have a dependence on the position x of the oscillator. Thus the effective potential of the oscillator has the form

$$\begin{aligned} V_{os\pm} &= \frac{1}{2}m\omega_0^2x^2 \pm \sqrt{\Delta^2 + (2gx - \epsilon)^2}, \\ V_{os_0} &= \frac{1}{2}m\omega_0^2x^2, \end{aligned} \quad (19)$$

where V_{os-} , V_{os+} and V_{os_0} correspond to the qubits in states $|g_1, g_2\rangle$, $|e_1, e_2\rangle$, and $|e_1, g_2\rangle$ (or $|g_1, e_2\rangle$), respectively.

Due to the correction terms in $V_{os\pm}$, when the qubits are in the same state, the effective potential of the oscillator is no longer harmonic, while it is the usual harmonic when the qubits are in opposite states. However, we can still obtain an approximate solution similarly to Ref. [19]

A renormalized frequency $\tilde{\omega}_0$ is obtained, which is given by

$$\begin{aligned} \tilde{\omega}_{0\pm}^2 &= \omega_0^2 \pm 4g^2/mE_q, \\ \tilde{\omega}_{0_0}^2 &= \omega_0^2, \end{aligned} \quad (20)$$

thus the relevant approximate effective potential is given by

$$\begin{aligned} V_{os\pm} &\approx \frac{1}{2}m\tilde{\omega}_{0\pm}^2 \left(x \mp \frac{2\epsilon g}{m\tilde{\omega}_{0\pm}^2 E_q} \right)^2 \pm E_q, \\ V_{os_0} &= \frac{1}{2}m\tilde{\omega}_{0_0}^2 x^2, \end{aligned} \quad (21)$$

It is interesting that the oscillator's frequency now has a dependence on the qubits' states, it increases when both of the qubits are in ground states, decreases when both of the qubits are in excited states, and stays unchanged when the qubits are in opposite states.

For V_{os+} , i.e., the qubits are both in excited states, the approximate effective potential is a displaced harmonic potential with an increased frequency, so the states of the oscillator

are displaced Fock states discussed in Sec. III.A. For V_{os_0} , i.e., the qubits are in opposite states, the effective potential is a usual harmonic potential, thus the oscillator's states are Fock states.

It is worthy to note that for V_{os_-} , the renormalized frequency $\tilde{\omega}_{0_-}$ turns into imaginary when $\omega_0^2 < 4g^2/mE_q$ (the stationary point), which means that under the condition

$$\frac{m\omega_0^2 E_q}{4g^2} < 1 \quad (22)$$

the system becomes unstable, and the approximate effective potential is not applicative any more as the effective potential becomes double-well. In the case of degeneracy point ($\epsilon = 0$), by differentiating V_{os_-} given in Eq. (19), one can obtain that the two minimal points of the double-well potential are located at $\pm x_0$, where $x_0 = \sqrt{4g^2/m^2\omega_0^4 - \Delta^2/4g^2}$. The energy barrier height between the two well is determined by $g^2/m\omega_0^2$. The effect of introducing a finite value of ϵ is that two wells are no longer symmetrical and the location of energy barrier is shifted to the left or right.

IV. CONCLUSION

In this paper we present a system that consists of two flux qubits coupled strongly to a transmission line oscillator, and obtain eigenenergies of the system and the properties of its eigenstates. Adiabatic approximation methods under two opposite extreme conditions, i.e., the adiabatic approximation in the displaced oscillator basis and the adiabatic approximation of the high-frequency qubits, which can be used to analyse our system are compared. Although they start by different assumptions, it has been proved that they are both valid in the ultrastrong coupling regime. There are some differences between these two approximations. It is notable that unlike the later approximation, there is no stationary point that turns harmonic potential into double-well potential in the former.

Acknowledgments - This work was supported by the NSFC (Grant No. 60978009), the Major Research Plan of the NSFC (Grant No. 91121023), and the SKPBR of China (Grant

- [1] A. Blais, R. S. Huang, A. Wallraff, S. M. Girvin, and R. J. Schoelkopf, *Phys. Rev. A* **69**, 062320 (2004).
- [2] Z. B. Feng, *Phys. Rev. A* **85**, 014302 (2012).
- [3] B. Peropadre, P. Forn-Díaz, E. Solano, and J. J. García-Ripoll, *Phys. Rev. Lett.* **105**, 023601 (2010).
- [4] J. Koch, T. M. Yu, J. Gambetta, A. A. Houck, D. I. Schuster, J. Majer, A. Blais, M. H. Devoret, S. M. Girvin, and R. J. Schoelkopf, *Phys. Rev. A* **76**, 042319 (2007).
- [5] G. Haack, F. Helmer, M. Mariani, F. Marquardt, and E. Solano, *Phys. Rev. B* **82**, 024514 (2010).
- [6] P. Nataf, and C. Ciuti, *Phys. Rev. Lett.* **104**, 023601 (2010).
- [7] P. Bushev, A. K. Feofanov, H. Rotzinger, I. Protopopov, J. H. Cole, C. M. Wilson, G. Fischer, A. Lukashenko, and A. V. Ustinov, *Phys. Rev. B* **84**, 060501 (2011).
- [8] J. Chen, J. B. Altepeter, M. Medic, K. F. Lee, B. Gokden, R. H. Hadfield, S. W. Nam, and P. Kumar, *Phys. Rev. Lett.* **100**, 133603 (2008).
- [9] C. P. Yang, S. I. Chu, and S. Han, *Phys. Rev. Lett.* **92**, 117902 (2004).
- [10] M. Hofheinz, E. M. Weig, M. Ansmann, R. C. Bialczak, E. Lucero, M. Neeley, A. D. O'Connell, H. Wang, J. M. Martinis, and A. N. Cleland, *Nature (London)* **454**, 310-314 (2008).
- [11] I. C. Hoi, C. M. Wilson, G. Johansson, T. Palomaki, B. Peropadre, and P. Delsing, *Phys. Rev. Lett.* **107**, 073601 (2011).
- [12] M. D. Reed, L. DiCarlo, B. R. Johnson, L. Sun, D. I. Schuster, L. Frunzio, and R. J. Schoelkopf, *Phys. Rev. Lett.* **105**, 173601 (2010).
- [13] Y. Makhlin, G. Schön, and A. Shnirman, *Rev. Mod. Phys.* **73**, 357 (2001).
- [14] S. Gustavsson, J. Bylander, F. Yan, W. D. Oliver, F. Yoshihara, and Y. Nakamura, *Phys. Rev. A* **84**, 014525 (2011).
- [15] J. Bourassa, J. M. Gambetta, A. A. A. Jr, O. Astafiev, Y. Nakamura, and A. Blais, *Phys. Rev. A* **80**, 032109 (2009).
- [16] E. K. Irish, *Phys. Rev. Lett.* **99**, 173601 (2007).
- [17] J. Casanova, G. Romero, I. Lizuain, J. J. García-Ripoll, and E. Solano, *Phys. Rev. Lett.* **105**,

263603 (2010).

[18] E. K. Irish, J. Gea-Banacloche, I. Martin, and K. C. Schwab, Phys. Rev. B **72**, 195410 (2005).

[19] S. Ashhab, and F. Nori, Phys. Rev. A **81**, 042311 (2010).